SCIENTIFIC PAPERS
OF THE UNIVERSITY OF PARDUBICE
Series A
Faculty of Chemical Technology
14 (2008)

WALL EFFECTS ON A SINGLE SPHERICAL PARTICLE MOVING THROUGH A POWER-LAW FLUID

Jaroslav STRNADEL and Ivan MACHAČ[1]
Department of Chemical Engineering,
The University of Pardubice, CZ–532 10 Pardubice

Received September 30, 2008

The steady motion of solid spheres through a power-law fluid contained in a cylindrical tube has been solved numerically using a finite element method by means of the COMSOL software package for the steady non-Newtonian flows. From the resulting stress fields, the drag force on the sphere, drag coefficient, drag coefficient corrective factor, and wall correction factor have been evaluated in dependence on the fluid power law index and the sphere-to-tube diameter ratio. The results of numerical computation are in very good agreement with previous theoretical and experimental literature data, which documents suitability of the computational method used.

[1] To whom correspondence should be addressed.

Introduction

The knowledge of the terminal velocity of particles falling in a viscous fluid is needed in a number of engineering applications such as solid-liquid separations, fluidization, solid transportation, rheometry, etc. Prediction of the terminal falling velocity is based on the knowledge of the drag coefficient of the flow around the particle. The calculation of the terminal falling velocity of a sphere moving through a Newtonian fluid is a classical problem and the drag coefficient correlations for a rigid spherical and non-spherical particles are described (especially for spherical particles) in a number of monographs and review papers (for example, Refs [1-3]). The influence of non-Newtonian behaviour on the drag coefficient of a sphere was more intensively investigated in the past several decades. The present-day scientific knowledge and the advances in particle motion in non-Newtonian media are reviewed in the book by Chhabra [4].

It is known that the confining walls or bounding surfaces caused an extra retardation effect on a falling particle due to an upward flux of the fluid displaced by the particle. On this account, the particle terminal velocity is reduced in comparison with that reached in the infinite medium. The particle retardation depends on the particle shape, orientation, and position, as well as on the fluid rheological behaviour, flow regime, and the geometry of the confining walls.

The particle retardation is customarily quantified using the wall correction factor f_W, which can be defined as the ratio of the terminal falling velocity of a particle in a bounded fluid to that in an unbounded one

$$f_W = \frac{U}{U_\infty} \tag{1}$$

The great deal of information on wall effects available in literature, especially for non-Newtonian fluids, concerns spherical particles and is based mainly on experiments. Only little theoretical and numerical work has been carried out on the effect of containing walls on sphere motion in purely viscous fluids without a yield stress [5]. Missirlis *et al.* [4,5] presented a numerical study of the wall effects on the terminal velocity of a sphere falling freely through a power-law fluid at the axis of a cylindrical tube in the creeping flow regime. Using both a finite-element and finite-volume method, they obtained results encompassing the ranges of power-law index $1 \geq n \geq 0.1$ and diameter ratio $0.50 \geq d/D \geq 0.02$. The wall effect is predicted to decrease with the decreasing values of n and d/D.

In this paper, the results are reported of our numerical solution of the flow of a power-law fluid over a solid sphere in a cylindrical tube in the creeping flow region, which have been obtained during the testing of the possibility to exploit the COMSOL software package for steady non-Newtonian flows to the solution

of the flow of purely viscous fluids around a solid obstacle. The results obtained are compared with available literature data.

Mathematical Model

We consider the flow of a power-law fluid around a sphere falling in an unbounded fluid and along the axis of a cylinder. The schematic representation of the domain used for the solution of the flow is shown in Fig. 1. For convenience, it is assumed that the sphere is held fixed and the cylinder walls are moving with the fluid velocity U.

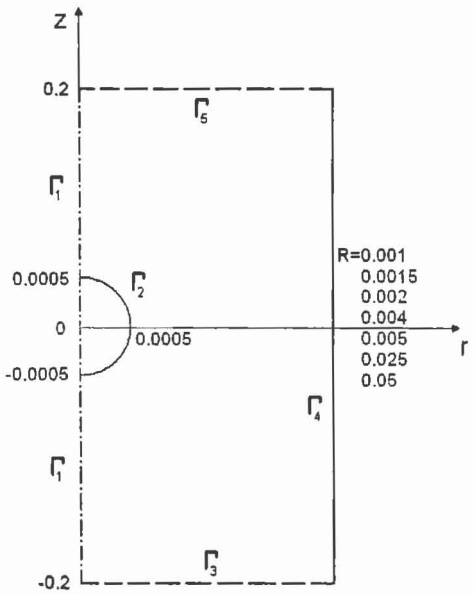

Fig.1 Schematic representation of the solution domain

The field equations governing the fluid motion are

continmuity equation	$\nabla\cdot\vec{u} = 0$	(2)
equation of motion	$\rho\vec{u}\cdot\nabla\vec{u} = -\nabla P + \nabla\cdot\vec{\vec{\tau}}$	(3)
constitutive equation	$\vec{\vec{\tau}} = \eta(\dot{\gamma})\vec{\vec{\gamma}}$	(4)
where	$\eta = K\dot{\gamma}^{n-1}$	(5)

Here $\vec{u}$ is the velocity vector, ρ the fluid density, P the pressure, $\vec{\vec{\tau}}$ the extra stress tensor, $\vec{\vec{\gamma}} = \nabla\vec{u} + \nabla\vec{u}^{\,T}$ the shear rate tensor, $\dot{\gamma} = \sqrt{\frac{1}{2}\vec{\vec{\gamma}}:\vec{\vec{\gamma}}}$ the shear rate, K the consistency, and n the power-law index.

For calculation, the two dimensional axial symmetric geometry with cylindrical coordinates (r, z) has been used. We have postulated the following boundary conditions for the flow solution in an unbounded fluid:

boundary Γ_1 – symmetry condition	$\vec{i}_r \cdot (-P\vec{\vec{I}} + \vec{\vec{\tau}}) \cdot \vec{i}_z = 0$	(6a)
	$\vec{i}_z \cdot \vec{u} = 0$	(6b)
boundaries Γ_4, Γ_5 – normal stress condition	$(-P\vec{\vec{I}} + \vec{\vec{\tau}}) \cdot \vec{i}_z = 0$	(6c)
boundary Γ_3 – velocity condition	$u_r = 0, \quad u_z = U$	(6d)
boundary Γ_2 – no slip condition	$\vec{u} = \vec{0}$	(6e)

For the flow solution in a bounded fluid, the boundary conditions on boundaries Γ_1, Γ_2, and Γ_5 remain the same. On the boundary Γ_3 the normal stress condition (6c) and on the boundary Γ_4 the velocity condition (6d) are valid.

The results of the numerical solution of the given mathematical model are the velocity, pressure, and stress fields. The quantities of interest are the drag force on the sphere

$$F_D = 2\pi \int_0^R \int_{-R}^{R} (P + \tau_{rz} + \tau_{zz}) \, dr \, dz \tag{7}$$

and the drag coefficient

$$c_D = \frac{|F_D|}{\pi R^2 \frac{1}{2} \rho U^2} \tag{8}$$

Analogously to Newtonian flow, the drag coefficient for the creeping flow of a power-law fluid around a sphere is commonly expressed as

$$c_D = \frac{24}{Re_n} X(n) \tag{9}$$

where $$Re_n = \frac{\rho U^{2-n} (2R)^n}{K} \tag{10}$$

is the generalised Reynolds number and $X(n)$ a drag coefficient corrective factor depending on the power-law index. From the comparison of Eq. (8) with Eq. (9), it follows that

$$X(n) = \frac{F_D}{6\pi K \left(\frac{U}{2R} \right)^{n-1} UR} \tag{11}$$

and the wall correction factor f_W, Eq. (1), is then given as

$$f_W = \left(\frac{X_\infty}{X} \right)^{\frac{1}{n}} \quad . \tag{12}$$

Solution Procedure

The governing equations (2) – (5) together with the boundary conditions (6) have been solved by a finite-element method based on the Galerkin formulation of the conservation equations.

The computations were performed with the computer programme COMSOL Multiphysics using software package for the steady non-Newtonian flows. Different triangular grids have been used for computation of different *d/D* ratios. On the boundary 2, the grid has been substantially refined. Table I shows number of grid elements and degrees of freedom used for the individual *d/D* ratios. The example of the grid used for calculation at $d/D = 0.33$ is shown in Fig. 2.

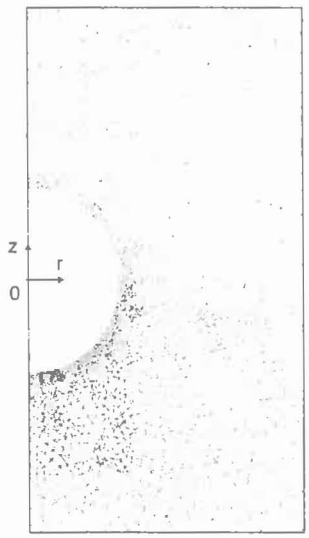

Fig. 2 Example of the grid used in the calculation with the ratio $d/D = 0.333$, number of elements 16 880

The UMFPACK direct solver has been used for index $n \in \langle 0.4, 1 \rangle$. The convergence of the computations has been rapidly falling for lower values of power-law index *n*. Hence, the use of the SPOOLES direct solver, which does not require so large contiguous memory blocks, has been necessary for the index $n \in \langle 0.1, 0.3 \rangle$.

Table I Number of elements and degrees of freedom used for the individual d/D ratios

d/D	Number of elements	D.O.F
0	45474	196739
0.01	26968	116877
0.02	19354	85815
0.1	36786	162739
0.125	20768	95551
0.25	23040	105463
0.333	16880	79413
0.4	19344	85771
0.5	19696	93285

Results and Discussion

Newtonian Fluid ($n = 1$)

The results of computation of Newtonian drag force have served as a check on suitability of the discretization scheme and boundary condition used. For $n = 1$, the dependence of the drag coefficient c_D on the Reynolds number in the range of Re from 0.001 to 200 for $d/D \to 0$, and the dependence of the wall correction factor f_W on the ratio d/D in the creeping flow region were calculated. In these calculations, the following values of entering quantities have been used: $d = 0.001$ m, $\rho = 1000$ kg m^{-3}, $U = 0.02$ or 0.04 m s^{-1}. The Reynolds number was changed by viscosity variation from 20 to 0.0002 Pa s.

The calculated dependence $c_D = f(Re)$ is displayed in Fig. 3. The computed values of c_D agree with an accuracy of 0.1 % with those determined numerically by Tabata and Itakura [6]. In Fig. 3, the computed data are compared with the well known Stokes solution

$$c_D = \frac{24}{Re} \tag{13}$$

which is useful for the creeping flow region ($Re < 0.1$), and with the simple empirical formulas of Schiller and Neumann [7]

$$c_D = \frac{24}{Re}\left(1 + 0.15 Re^{0.687}\right) \tag{14}$$

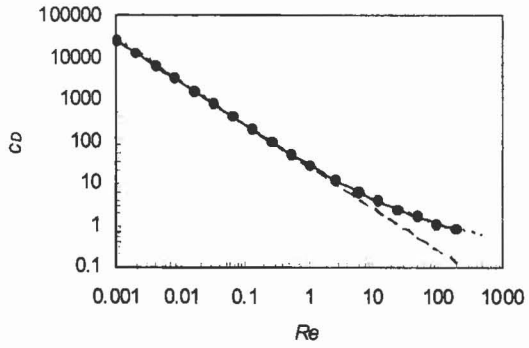

Fig. 3 Dependence of the drag coefficient c_D on the Reynolds number Re: • – calculated data; – – – – Eq. (13); —— – Eq. (14); ····· – Eq. (15)

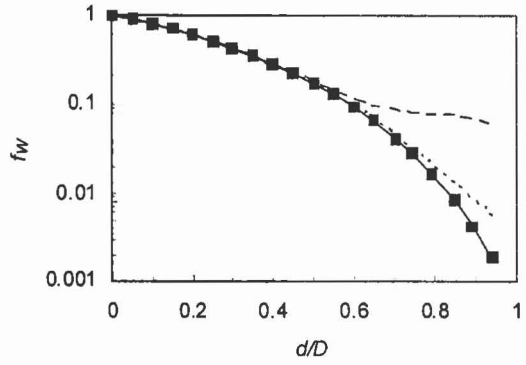

Fig. 4 Dependence of the wall correction factor f_W on the ratio d/D for the creping flow region. ■ – calculated data; – – – – Eq. (16); ····· – Eq. (17); —— – Eq. (18)

which is recommended for $0.2 < Re < 500 - 1000$, and Khan and Richardson [3,4]

$$c_D = \left(2.25 Re^{-0.31} + 0.36 Re^{0.06}\right)^{3.45} \tag{15}$$

which predicts the drag coefficient with an average uncertainty of less than 5 % in the range of $10^{-2} < Re < 3 \times 10^5$. Very good agreement between numerically calculated data of c_D and those presented by Tabata and Itakura [6] and those determined at low values of Re from Eq. (13) and at higher values of Re according to eqs. (14) and (15) bears evidence of the suitability of the solution procedure used.

The computed dependence $f_W = f(d/D)$ is displayed in Fig. 4. It was compared with the dependences evaluated from the classical correlation of Faxen [4]

$$f_W = 1 - 2.104\frac{d}{D} + 2.09\left(\frac{d}{D}\right)^3 - 0.95\left(\frac{d}{D}\right)^5 \qquad (16)$$

which is limited to low values of the d/D ratio, and from the relationship of Haberman and Sayre [1,4]

$$f_W = \frac{1 - 2.105\frac{d}{D} + 2.0865\left(\frac{d}{D}\right)^3 - 1.706\left(\frac{d}{D}\right)^5 + 0.72603\left(\frac{d}{D}\right)^6}{1 - 0.75857\left(\frac{d}{D}\right)^5} \qquad (17)$$

which is stated to be valid in the range $0 \le \frac{d}{D} \le 0.80$. Figure 4 shows that the relationship (16) approximates the computed data of f_W with a sufficient accuracy up to $d/D = 0.5$ and the relationship (17) up to $d/D = 0.7$. It has been found that the computed dependence $f_W = f(d/D)$ can be approximated with the same good accuracy by the polynomial

$$f_W = 1 - 1.943\frac{d}{D} - 1.290\left(\frac{d}{D}\right)^2 + 6.594\left(\frac{d}{D}\right)^3 - 7.690\left(\frac{d}{D}\right)^4 + 4.528\left(\frac{d}{D}\right)^5 - 1.200\left(\frac{d}{D}\right)^6 \qquad (18)$$

up to $\frac{d}{D} = 0.94$.

Power-law Fluid

For $n < 1$, the dependences $X = X(d/D, n)$ and $f_W = f(d/D, n)$ were evaluated in the creeping flow region. In the drag force F_D calculations, the following values of entering quantities were used: $d = 0.001$ m, $\rho = 1000$ kg m^{-3}, $U = 0.02$ m s^{-1}, $K =$ 1 Pa s^n, $0.1 \le n \le 1$, $0 \le \frac{d}{D} \le 0.5$.

The computed values of the corrective factor X are summarized in Table II. Their agreement with the values of X determined numerically by Missirlis *et al.* [5] is, especially for $n < 0.9$, very good. The mean relative deviation between data of X calculated in this work and the corresponding data determined by Missirlis

Table II Computed values of the drag coefficient corrective factor X

n	d/D								
	0	0.01	0.02	0.1	0.125	0.25	0.333	0.4	0.5
1	1.0006	1.0164	1.0358	1.2513	1.3363	1.9524	2.6527	3.5153	5.7667
0.9	1.1374	1.1455	1.1572	1.3211	1.3912	1.9115	2.4991	3.2096	5.0089
0.8	1.2575	1.2607	1.2668	1.3825	1.4377	1.8629	2.3448	2.9186	4.3321
0.7	1.3553	1.3564	1.3591	1.4336	1.4744	1.8075	2.1915	2.6442	2.7325
0.6	1.4288	1.4289	1.4299	1.4721	1.4999	1.7463	2.0409	2.3879	3.2060
0.5	1.4759	1.4758	1.4761	1.4957	1.5125	1.6801	1.8946	2.1501	2.7469
0.4	1.4951	1.4949	1.4951	1.5011	1.5098	1.6094	1.7531	1.9306	2.3480
0.3	1.4838	1.4834	1.4836	1.4832	1.4873	1.5333	1.6164	1.7281	2.0013
0.2	1.4360	1.4354	1.4356	1.4329	1.4363	1.4484	1.4826	1.5405	1.6985
0.1	1.3414	1.3393	1.3400	1.3359	1.3413	1.3421	1.3444	1.3622	1.4301

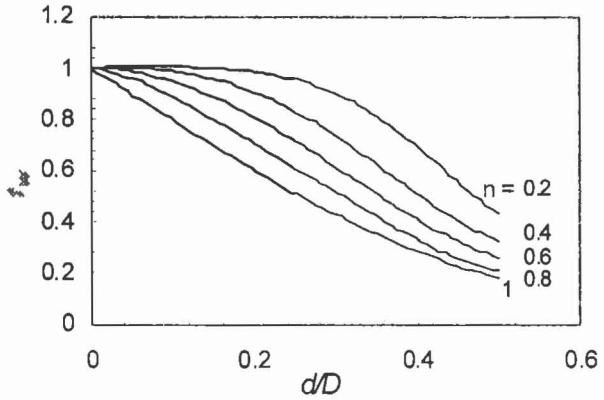

Fig. 5 Calculated dependences of f_W on d/D for parametric values of n.

et al. [5] is only 0.42 %. The maximum deviation achieved for $n = 1$ and $d/D = 0.5$ is 3 %.

Using the data of X given in Table II, the values of the wall corrective factor f_W were calculated according to Eq. (12). The examples of the obtained dependences $f_W = f(d/D, n)$ are shown in Fig. 5. These dependences are nearly identical with those based on the results of Missirlis *et al.* [5], which are given in Fig. 10.5 in Chhabra's book [4].

The wall correction factor is approaching to the value of $f_W = 1$ for $d/D \to 0$. For $d/D > 0$, the value of f_W gradually goes down bellow unity in dependence on

the index n. At the same time, the wall corrective factor reduction is slower with decreasing value of n. The theoretical course of the dependence $f_W = f(d/D, n)$ (Fig. 5) can be approximated in the range $0.5 \leq \frac{d}{D} \leq 1$ by the relationship

$$f_W = \frac{1}{1 + k_1 \frac{d}{D} + k_2 \left(\frac{d}{D}\right)^2 + k_3 \left(\frac{d}{D}\right)^3 + k_4 \left(\frac{d}{D}\right)^4} \tag{19}$$

where the dependences of parameters k_1-k_5 on the flow index n are given by the following polynomial functions

$$k_1 = a_1 n^2 + a_2 n, \tag{20a}$$
$$k_2 = a_1 n^2 + a_3 n + a_3, \tag{20b}$$
$$k_3 = a_4 n^2 - a_4 n + a_5, \tag{20c}$$
$$k_4 = a_6 n^2 + a_4 n - a_4. \tag{20d}$$

The mean relative deviation between numerically calculated data of f_W and those calculated according to Eq. (19), using parameters a_1- a_6 summarized in Table III, is only 1.2 %. The maximum deviation is 2.7 %.

Table III Parameters a_i (i = 1, 2, ... 6) in Eq. (20)

a_1	a_2	a_3	a_4	a_5	a_6
4.317	–2.963	4.827	–66.09	–38.80	84.44

The theoretical functional dependence $f_W = f(d/D, n)$ was collated with available experimental data by Chhabra [4]. He affirms that the flow index n seems to exert virtually no influence on the extent of wall effects in power-law fluids, and the wall factor varies linearly with the diameter ratio as

$$f_W = 1 + A \frac{d}{D} \tag{21}$$

Most of the literature data covering $0.52 \leq n \leq 0.95$, $0 \leq \frac{d}{D} \leq 0.5$ are well correlated with a single value of $A = 1.6$. At the same time, the wall effects are seen to be smaller in power fluids than those in Newtonian media. These statements have also been acknowledged, at least for $d/D < 0.25$, by the results of our previous experiments in the creeping flow region [8]. In these experiments, the terminal falling velocities were measured with glass, steel, and lead spherical par-

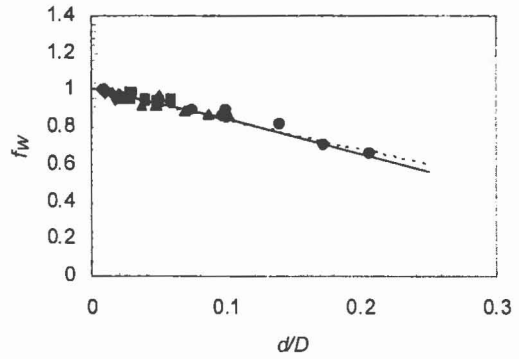

Fig. 6a Wall correction factor versus sphere-to-tube diameter ratio for fall in 2.5 % solution of Cellosize QP-40, $n = 0.935$. Bold symbols, experiments; ····· – Eq. (20); —— – numerical calculation

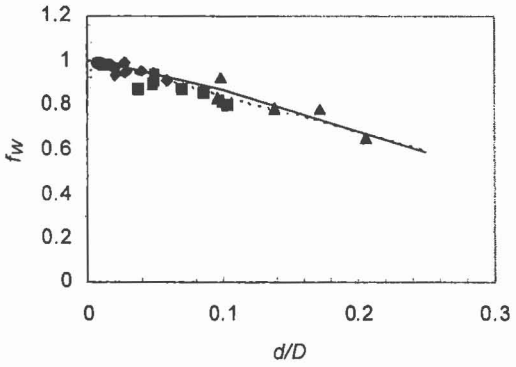

Fig. 6b Wall correction factor versus sphere-to-tube diameter ratio for fall in 1.3 % solution of Natrosol 250 MR, $n = 0.844$. Bold symbols, experiments; ····· – Eq. (20); —— – numerical calculation

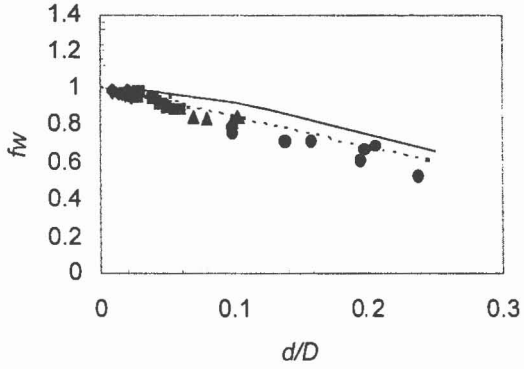

Fig. 6c Wall correction factor versus sphere-to-tube diameter ratio for fall in 1.3 % solution of Natrosol 250 H, $n = 0.672$. Bold symbols, experiments; ····· – Eq. (20); —— – numerical calculation.

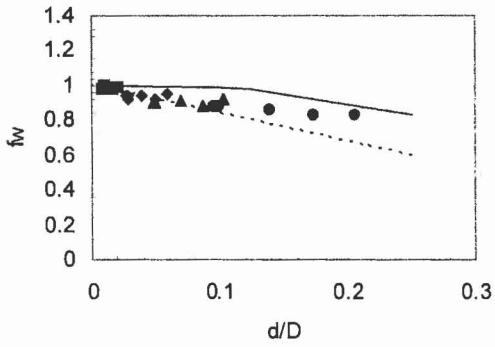

Fig. 6d Wall correction factor versus sphere-to-tube diameter ratio for fall in 0.5 % solution of Separan AP 45, n = 0.369. Bold symbols, experiments; ····· – Eq. (20); —— – numerical calculation

ticles moving through different shear thinning polymer solutions in cylindrical columns of 200, 70, 40, and 20 mm in diameter. The diameter of spheres ranged from 1.46 mm to 4.75 mm. The resulting experimental dependences $f_W = f(d/D)$ are shown for the fall in the 2.5 % solution of hydroxyethylcellulose Cellosize QP-40,1.3 % solution of hydroxyethylcellulose Natrosol 250 MR, 1.3 % solution of hydroxy-ethylcellulose Natrosol 250 H, and 0.5 % solution of polyacrylamide Separan AP 45 in Figs 6a-6d.

Figures 6a-6c show that a satisfactory correspondence between experimental data f_W and those predicted according to Eq. (21) with A = 1.6 exists. At the same time, the deviations between f_W data predicted according to Eq. (21) and those calculated numerically (Fig. 5) do not exceed, for $0.7 \leq n \leq 0.95$, the errors of experimental determination of f_W. On the other hand, Fig. 6d shows that, at low value of n = 0.369, Eq. (21) yields, for $d/D > 0.12$, lower values of f_W in comparison with the experimental data. The experiments are better approximated with the numerical solution presented in this work. Since there is a lack of available literature data on the wall effects in the fall of spherical particles through highly shear thinning fluids, it will be suitable to perform other experiments in this area.

Conclusion

A numerical solution of the steady motion of solid spheres through a power-law fluid contained in a cylindrical tube has been presented. The given mathematical model of the flow around a sphere has been solved using a finite element method by means of the COMSOL software package for the steady non-Newtonian flows. The quantities of interest were the drag force F_D on the sphere, drag coefficient c_D,

drag coefficient corrective factor X, and wall correction factor f_W, which were evaluated on the basis of resulting stress fields.

For $n = 1$ (Newtonian fluid), the dependence of the drag coefficient c_D on the Reynolds number in the range of Re from 0.001 to 200 for d/D → 0, and the dependence of the wall correction factor f_W on the ratio d/D in the creeping flow region were calculated. The results obtained for $n = 1$ are in very good agreement with the published theoretical and experimental data.

For $n < 1$, the dependences $X = X(d/D, n)$ and $f_W = f(d/D, n)$ were evaluated in the creeping flow region. It was shown that the numerically calculated dependences of the wall correction factor f_W on the ratio d/D and flow index n can be approximated with very good accuracy by the proposed equations (19) and (20). The numerical results indicate that the retardation effect of the walls on the terminal falling velocity of particles decreases with the increasing shear thinning of the fluid. This fact contrasts with the experimental findings that the flow index has no significant influence on the value of f_W, at least in the range $0.5 \leq n \leq 1$. Therefore, it will be suitable to perform other experiments in this area.

Symbols

a_i	($i = 1, 2, \ldots 6$) parameters in Eqs (20)
c_D	drag coefficient
d	sphere diameter, m
D	tube diameter, m
f_W	wall correction factor defined by Eq. (1)
$\vec{i}$	unit vector
$\vec{\vec{I}}$	unit tensor
k_i	($i = 1, 2, \ldots 4$) parameters in Eq. (19)
K	power-law parameter (consistency coefficient), Pa s^n
P	pressure, Pa
r	radial cylindrical coordinate, m
R	sphere radius, m
Re	Reynolds number
Re_n	power-law Reynolds number, Eq. (10)
u	velocity vector component, m s^{-1}
$\vec{u}$	velocity vector, m s^{-1}
U	particle terminal falling velocity, m s^{-1}
X	drag coefficient corrective factor
z	axial cylindrical coordinate, m
$\dot{\gamma}$	shear rate, s^{-1}
$\vec{\vec{\dot{\gamma}}}$	shear rate tensor, s^{-1}
η	viscosity of non-Newtonian liquid, Pa s

μ dynamic viscosity, Pa s
ρ fluid density, kg m^{-3}
τ extra stress tensor component
$\overleftrightarrow{\tau}$ extra stress tensor, Pa

Subscripts

r related to the radial cylindrical component
z related to the axial cylindrical component
∞ related to the unbounded fluid

Acknowledgements

The authors thank the Grant Agency of the Czech Republic for financial support of this work (Grant project No. 104/08/H055).

References

[1] Happel J., Brenner H.: *Low Reynolds Number Hydrodynamics*, Prentice-Hall, Inc., Englewood Cliffs, N. J. 1965.
[2] Clift R., Grace J.R., Weber M.E.: *Bubbles, Drops, and Particles,* Academic Press, New York 1978.
[3] Khan A.R., Richardson J.F.: Chem. Eng. Commun. **62**, 135 (1987).
[4] Chhabra R.P.: *Bubbles, Drops, and Particles in Non-Newtonian Fluids*, 2nd edition, CRC Press, Boca Raton, FL, 2006.
[5] Missirlis K.A., Assimacopoulos D., Mitsoulis E., Chhabra R.P.: J. Non-Newtonian Fluid Mech. **96**, 459 (2001).
[6] Tabata M., Itakura K.: Int. J. Comp. Fluid Dyn. **9**, 303 (1998).
[7] Schiller L., Naumann A.: Z. Ver Deut. Ing. **77**, 318 (1933).
[8] Ullrich P.: *Fall of Spherical Particle in Non-Newtonian Fluid* (in Czech), Diploma Thesis. Institute of Chemical Technology, Pardubice, 1982.